Supplement of Atmos. Chem. Phys., 19, 11635–11649, 2019
https://doi.org/10.5194/acp-19-11635-2019-supplement

*Supplement of*

# Investigation of the $\alpha$-pinene photooxidation by OH in the atmospheric simulation chamber SAPHIR

**Michael Rolletter et al.**

*Correspondence to:* Hendrik Fuchs (h.fuchs@fz-juelich.de)

## S1 Calculation of product yields

To calculate the yield as described in Galloway et al. (2011) and Kaminski et al. (2017) it is necessary to correct measured concentrations for losses and additional sources. The correction term for the example of pinonaldehyde is shown in Eq. S1:

$$c_{\text{pinal corr}}[i] = c_{\text{pinal}}[i-1] + \Delta c_{\text{pinal}} + \Delta c_{\text{dil}} + \Delta c_{\text{rl}} + \Delta c_{\text{pl}} - \Delta c_{\text{O3}} \tag{S1}$$

To obtain the corrected pinonaldehyde concentration $c_{\text{pinal corr}}$ the measured concentration $c_{\text{pinal}}$ has to be corrected for losses by photolysis $\Delta c_{\text{pl}}$, dilution $\Delta c_{\text{dil}}$ and the reaction with OH radicals $\Delta c_{\text{rl}}$, as well as a source from the ozonolysis of $\alpha$-pinene $\Delta c_{\text{O3}}$. The different terms are further explained in the equations S2 to S5:

$$\Delta c_{\text{dil}} = c_{\text{pinal}}[i-1] * \Delta t * k_{\text{dil}}[i-1] \tag{S2}$$

$$\Delta c_{\text{rl}} = c_{\text{pinal}}[i-1] * \Delta t * c_{\text{OH}}[i-1] * k_{\text{pinal + OH}} \tag{S3}$$

$$\Delta c_{\text{pl}} = c_{\text{pinal}}[i-1] * \Delta t * J_{\text{pinal}}[i-1] \tag{S4}$$

$$\Delta c_{\text{O3}} = c_{\text{pinal}}[i-1] * \Delta t * c_{\text{O3}}[i-1] * k_{\text{apinene + O3}} \tag{S5}$$

$c_{\text{pinal corr}}[i]$ : corrected pinonaldehyde concentration at time *i*

$c_{\text{pinal}}[i-1]$ : measured pinonaldehyde concentration at time *i*-1

$\Delta c_{\text{dil}}$ : dilution

$\Delta c_{\text{rl}}$ : loss due to the reaction with OH

$\Delta c_{\text{pl}}$ : photolytic loss

$\Delta c_{\text{O3}}$ : production from ozonolysis

$c_{\text{OH}}[i-1]$ : measured OH concentration by DOAS at time *i*-1

$k_{\text{pinal + OH}}$ : reaction rate of pinonaldehyde + OH (Atkinson et al., 2006)

$J_{\text{pinal}}[i-1]$ : measured photolysis frequency at time *i*-1

$c_{\text{O3}}[i-1]$ : $O_3$ concentration at time *i*-1

$k_{\text{apinene + O3}}$ : reaction rate of $\alpha$-pinene + $O_3$ (MCM, 2019)

An overview of all corrections made for the different species is shown in Table S1.

Fig. S1 shows the measured (blue) and corrected concentrations (red). For $\alpha$-pinene the amount of reacted substance is accumulated over the whole duration of the experiment and corrected for losses by ozonolysis and dilution. The corrected HCHO, acetone and pinonaldehyde are then plotted versus the corrected amount of reacted $\alpha$-pinene. The yield of the reaction $\alpha$-pinene + OH is derived from the resulting slopes.

|  | corrected for |  |
|---|---|---|
| species | losses by | sources from |
| $\alpha$-pinene | $\alpha$-pinene + $O_3$<br>dilution | / |
| pinonaldehyde | pinonaldehyde + h$\nu$<br>pinonaldehyde + OH<br>dilution | $\alpha$-pinene + $O_3$ |
| acetone | acetone + OH<br>dilution | chamber wall |
| HCHO | HCHO + OH<br>HCHO + h$\nu$<br>dilution | $CH_3CHO$ + OH<br>chamber wall |

**Table S1.** Overview of correction terms for the analysed species applied in the yield calculation.

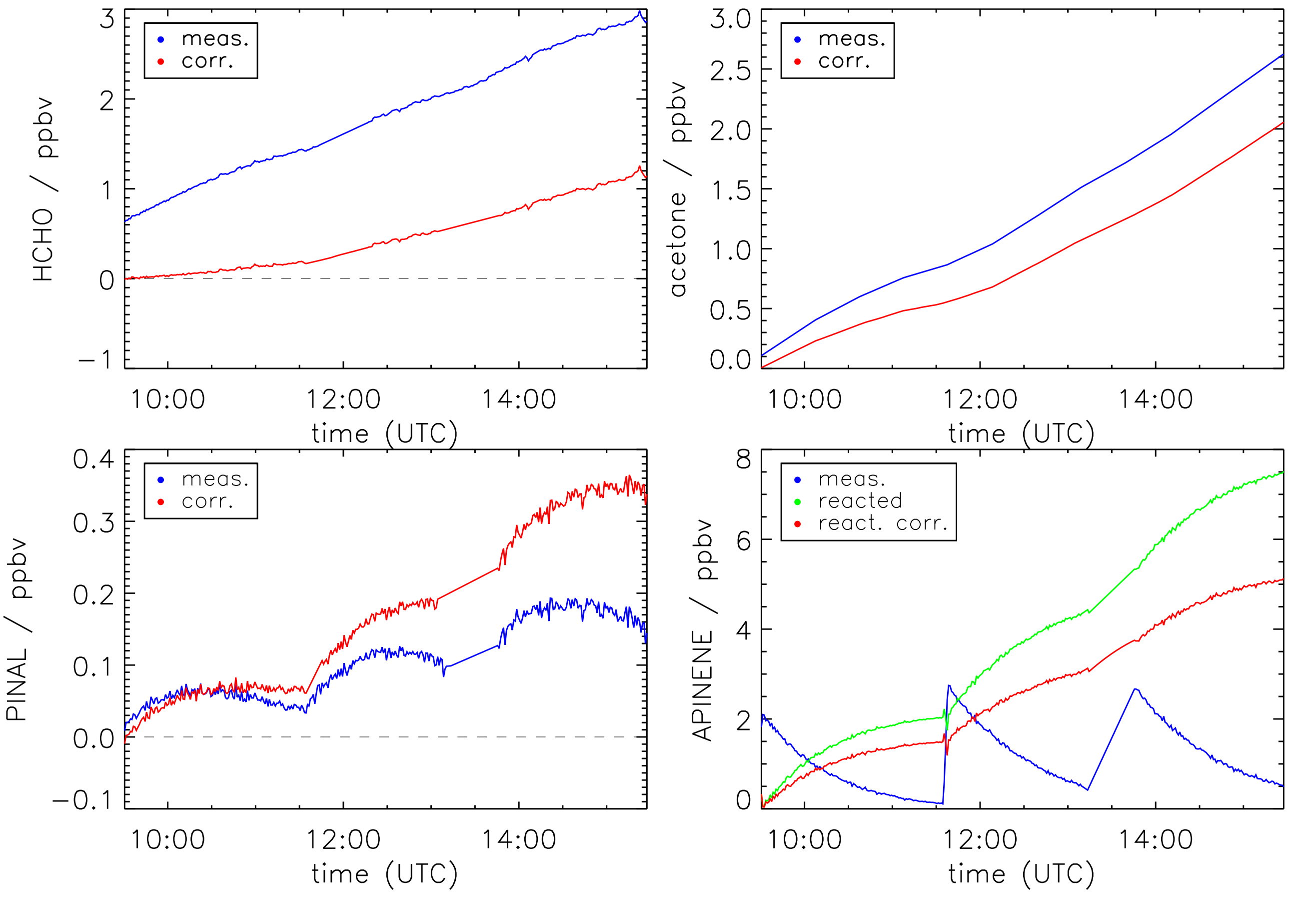

**Figure S1.** The blue curves show the measured concentrations. For $\alpha$-pinene the green curve represents the amount of reacted substance. The individual concentrations after the applied correction are shown in red.

## S2 Model modifications for M1 sensitivity study

All additions made in the sensitivity run M1 based on the suggestions by Vereecken et al. (2007) are shown in Tables S2 and S3. The naming schema of reactants starting with an "R" is according to Vereecken et al. (2007). Table S2 shows the initial oxidation step of the $\mathrm{OH}$ attack, and the subsequent chemistry of the $\mathrm{RO_2}$ after the $\mathrm{OH}$ addition.

For simplification only one out of three hydrogen-abstraction pathways is included here forming compound $\mathrm{ROOA}$. The subsequent chemistry of $\mathrm{ROOA}$ is shown in Table S3.

$\mathrm{APINCO2}$ was replaced by $\mathrm{synR1}$ and $\mathrm{antiR1}$ as the mechanism by Vereecken et al. (2007) distinguishes the syn and anti stereoisomers of this compound following different pathways. Both $\mathrm{synR1}$ and $\mathrm{antiR1}$ can react with $\mathrm{NO}$ but this pathway is outrun by the unimolecular reactions 1,6-H shift, which is only happening for anti isomer, and the ring-closure forming R4. The late degradation products after the 1,6-H-shift are 8-OOH-menthen-6-one (R7P1) and 2-OH-OOH-menthen-6-one (R9P1). The ring-closure leads to the formation of a dicarbonyl cycloperoxide (R5P1).

The model introduced new $\mathrm{RO_2}$, which are not been part of the MCM, and a substantial fraction of the total reaction procedes through these pathways. This underestimates the $\mathrm{HO_2}$ loss by the reaction of $\mathrm{RO_2}$ + $\mathrm{OH}$, especially in the sensitivity run M2. Therefore the $\mathrm{RO_2}$ + $\mathrm{HO_2}$reactions in the lower half of Table S3 are added.

**Table S2.** Additional and modified reactions applied to the MCM based on the proposed mechanism by Vereecken et al. (2007). For additional OH abstraction chemistry see Table S3. All nitrate species are lumped as one species RNO3.

| reaction | reaction rate constant |
|---|---|
| APINENE + OH→ROOA | $0.12 \times 1.2 \times 10^{-11} \exp(440\mathrm{K}/\mathrm{T})\,\mathrm{cm}^3\mathrm{s}^{-1}$ |
| APINENE + OH→APINAO2 | $0.22 \times 1.2 \times 10^{-11} \exp(440\mathrm{K}/\mathrm{T})\,\mathrm{cm}^3\mathrm{s}^{-1}$ |
| APINENE + OH→APINBO2 | $0.44 \times 1.2 \times 10^{-11} \exp(440\mathrm{K}/\mathrm{T})\,\mathrm{cm}^3\mathrm{s}^{-1}$ |
| APINENE + OH→synR1 | $0.4 \times 0.22 \times 1.2 \times 10^{-11} \exp(440\mathrm{K}/\mathrm{T})\,\mathrm{cm}^3\mathrm{s}^{-1}$ |
| APINENE + OH→antiR1 | $0.6 \times 0.22 \times 1.2 \times 10^{-11} \exp(440\mathrm{K}/\mathrm{T})\,\mathrm{cm}^3\mathrm{s}^{-1}$ |
| APINAO2 + NO→APINANO3 | $0.03\times$ KRO2NO[a] |
| APINAO2 + NO→APINAO + NO2 | $0.97\times$ KRO2NO[a] |
| APINAO →PINAL + HO2 | $0.875\times$ KDEC[b] |
| APINAO →HCHO + HO2 | $0.125\times$ KDEC[b] |
| APINBO2 + NO→APINBNO3 | $0.07\times$ KRO2NO[a] |
| APINBO2 + NO→APINBO + NO2 | $0.93\times$ KRO2NO[a] |
| antiR1 + NO →R2 + NO2 | KRO2NO[a] |
| antiR1 →R4 | $0.6\,\mathrm{s}^{-1}$ |
| antiR1 →R7 | $11.5\,\mathrm{s}^{-1}$ |
| synR1 + NO→R2 + NO2 | KRO2NO[a] |
| synR1 →R4 | $2.6\,\mathrm{s}^{-1}$ |
| R2 →R2P1 + CH3COCH3 + HO2 | KDEC[b] |
| R4 + NO→RNO3 | $0.1\times$ KRO2NO[a] |
| R4 + NO→R5 + NO2 | $0.9\times$ KRO2NO[a] |
| R5 →R5P1 + HO2 | KDEC[b] |
| R7 →R8 | $0.5\times$ KDEC[b] |
| R7 →R7P1 + HO2 | $0.5\times$KDEC[b] |
| R8 + NO→RNO3 | $0.29\times$ KRO2NO[a] |
| R8 + NO→R9 + NO2 | $0.71\times$ KRO2NO[a] |
| R9 →R9P1 + HO2 | KDEC[b] |

[a] value from MCM: KRO2NO= $2.7 \times 10^{-12} \exp(360\mathrm{K}/\mathrm{T})\,\mathrm{cm}^3\mathrm{s}^{-1}$ (MCM, 2019)

[b] value from MCM: KDEC= $1.0 \times 10^6$ (MCM, 2019)

**Table S3.** Additional OH abstraction reactions and subsequent product reactions applied to the MCM based on the proposed mechanism by Vereecken et al. (2007). All nitrate species are lumped as one species RNO3. All reaction products of $RO_2 + HO_2$ are lumped as one species RRO2.

| reaction | reaction rate constant |
|---|---|
| $\mathrm{ROOA + NO \rightarrow RNO3}$ | $0.11\times$ KRO2NO[a] |
| $\mathrm{ROOA + NO \rightarrow ROA + NO2}$ | $0.89\times$ KRO2NO[a] |
| $\mathrm{ROA \rightarrow ROOB}$ | $0.6\times$ KDEC[b] |
| $\mathrm{ROA \rightarrow ROOC}$ | $0.4\times$ KDEC[b] |
| $\mathrm{ROOB + NO \rightarrow RNO3}$ | $0.11\times$ KRO2NO[a] |
| $\mathrm{ROOB + NO \rightarrow ROB + NO2}$ | $0.89\times$ KRO2NO[a] |
| $\mathrm{ROB \rightarrow CH3COCH3 + HCHO + HO2}$ | KDEC[b] |
| $\mathrm{ROOC + NO \rightarrow RNO3}$ | $0.11\times$ KRO2NO[a] |
| $\mathrm{ROOC + NO \rightarrow ROC + NO2}$ | $0.89\times$ KRO2NO[a] |
| $\mathrm{ROC \rightarrow HCHO + HO2}$ | KDEC[b] |
| $\mathrm{synR1 + HO2 \rightarrow APINCOOH}$ | KRO2HO2[c] |
| $\mathrm{antiR1 + HO2 \rightarrow APINCOOH}$ | KRO2HO2[c] |
| $\mathrm{R4 + HO2 \rightarrow RRO2}$ | KRO2HO2[c] |
| $\mathrm{R8 + HO2 \rightarrow RRO2}$ | KRO2HO2[c] |
| $\mathrm{R10 + HO2 \rightarrow RRO2}$ | KRO2HO2[c] |
| $\mathrm{R12 + HO2 \rightarrow RRO2}$ | KRO2HO2[c] |
| $\mathrm{ROOA + HO2 \rightarrow RRO2}$ | KRO2HO2[c] |
| $\mathrm{ROOB + HO2 \rightarrow RRO2}$ | KRO2HO2[c] |
| $\mathrm{ROOC + HO2 \rightarrow RRO2}$ | KRO2HO2[c] |

[a] value from MCM: KRO2NO$= 2.7\times10^{-12}\,\exp(360\mathrm{K}/\mathrm{T})\,\mathrm{cm^3 s^{-1}}$ (MCM, 2019)

[b] value from MCM: KDEC$= 1.0\times10^{6}$ (MCM, 2019)

[c] value from MCM: KRO2HO2$= 2.91\times10^{-13}\,\exp(1300\mathrm{K}/\mathrm{T})\,\mathrm{cm^3 s^{-1}}$ (MCM, 2019)

## S3 Sensitivity study for Xu et al.

Xu et al. (2019) studied the reaction $\alpha$-pinene + OH and proposed a mechanism constrained by experimentally determined hydroxynitrates yields. An overall shift in the initial $RO_2$ distribution towards APINCO2 was proposed. We performed an additional sensitivity run based on M1 with the proposed initial $RO_2$ distribution for APINAO2/APINBO2/APINCO2 of 0.02/0.28/0.60 and 0.10 for H-abstraction reactions. The results are shown in Fig. S2. The pinonaldehyde production is lowered by 50 % compared to M1, but is still overestimating the measured pinonaldehyde concentration by a factor of 3. The additional pinonaldehyde is derived from the higher APINBO2 fraction of 28 % compared to 5 % in M2. The formation of formaldehyde is well reproduced. In contrast, the model underpredicts the acetone production, similar to M2, but with a smaller model-measurement discrepancy of 15 %. The agreement of modeled OH and $HO_2$ concentrations is around 10 % lower compared to M2, but both agree with the measurements within the stated uncertainty

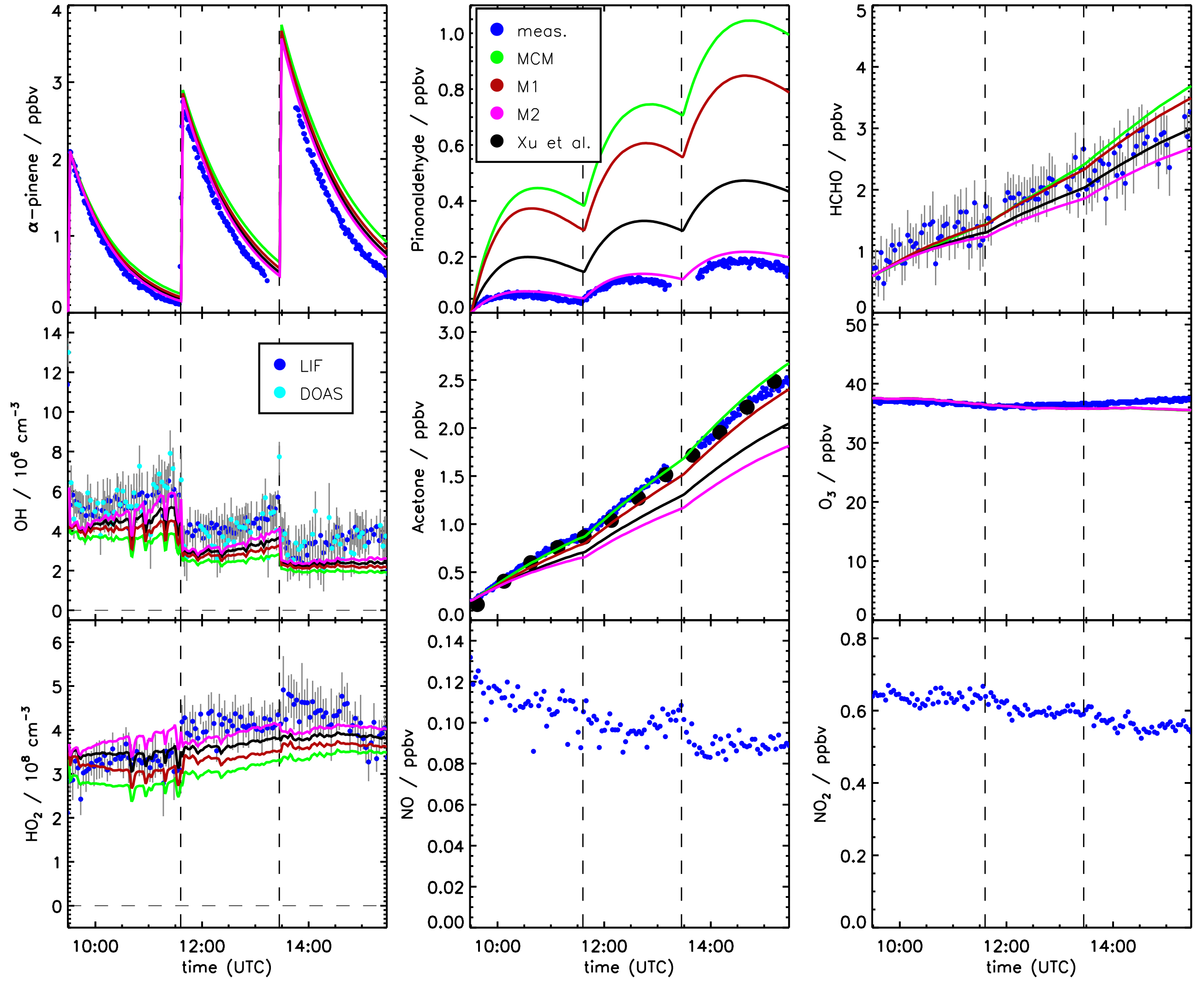

**Figure S2.** Time series of measured and modelled concentrations of radicals, inorganic and organic compounds during the $\alpha$-pinene photooxidation at low NO (experiment on 02 July 2014).

## References

Atkinson, R., Baulch, D. L., Cox, R. A., Crowley, J. N., Hampson, R. F., Hynes, R. G., Jenkin, M. E., Rossi, M. J., Troe, J., and Subcommittee, I.: Evaluated kinetic and photochemical data for atmospheric chemistry: Volume II - gas phase reactions of organic species, Atmos. Chem. Phys., 6, 3625–4055, https://doi.org/10.5194/acp-6-3625-2006, 2006.

Galloway, M. M., Huisman, A. J., Yee, L. D., Chan, A. W. H., Loza, C. L., Seinfeld, J. H., and Keutsch, F. N.: Yields of oxidized volatile organic compounds during the OH radical initiated oxidation of isoprene, methyl vinyl ketone, and methacrolein under high-$NO_X$ conditions, Atmos. Chem. Phys., 11, 10 779–10 790, https://doi.org/10.5194/acp-11-10779-2011, 2011.

Kaminski, M., Fuchs, H., Acir, I. H., Bohn, B., Brauers, T., Dorn, H. P., Häseler, R., Hofzumahaus, A., Li, X., Lutz, A., Nehr, S., Rohrer, F., Tillmann, R., Vereecken, L., Wegener, R., and Wahner, A.: Investigation of the $\beta$-pinene photooxidation by OH in the atmosphere simulation chamber SAPHIR, Atmos. Chem. Phys., 17, 6631–6650, https://doi.org/10.5194/acp-17-6631-2017, 2017.

MCM: The Master Chemical Mechanism, v3.3.1, http://mcm.leeds.ac.uk/MCM, last access: 28 April, 2019.

Vereecken, L., Müller, J. F., and Peeters, J.: Low-volatility poly-oxygenates in the OH-initiated atmospheric oxidation of $\alpha$-pinene: impact of non-traditional peroxyl radical chemistry, Phys. Chem. Chem. Phys., 9, 5241–5248, https://doi.org/10.1039/B708023A, 2007.

Xu, L., Møller, K. H., Crounse, J. D., Otkjær, R. V., Kjaergaard, H. G., and Wennberg, P. O.: Unimolecular Reactions of Peroxy Radicals Formed in the Oxidation of $\alpha$-Pinene and $\beta$-Pinene by Hydroxyl Radicals, J. Phys. Chem. A,, 123, 1661–1674, https://doi.org/10.1021/acs.jpca.8b11726, 2019.